

# Search-based Path Planning for a High Dimensional Manipulator in Cluttered Environments Using Optimization-based Primitives

Muhammad Suhail Saleem<sup>1</sup>, Raghav Sood<sup>1</sup>, Sho Onodera<sup>2</sup>, Rohit Arora<sup>2</sup>,  
Hiroyuki Kanazawa<sup>2</sup>, and Maxim Likhachev<sup>1</sup>

**Abstract**—In this work we tackle the path planning problem for a 21-dimensional snake robot-like manipulator, navigating a cluttered gas turbine for the purposes of inspection. Heuristic search based approaches are effective planning strategies for common manipulation domains. However, their performance on high dimensional systems is heavily reliant on the effectiveness of the action space and the heuristics chosen. The complex nature of our system, reachability constraints, and highly cluttered turbine environment renders naive choices of action spaces and heuristics ineffective. To this extent we have developed i) a methodology for dynamically generating actions based on online optimization that help the robot navigate narrow spaces, ii) a technique for lazily generating these computationally expensive optimization actions to effectively utilize resources, and iii) heuristics that reason about the homotopy classes induced by the blades of the turbine in the robot workspace and a Multi-Heuristic framework which guides the search along the relevant classes. The impact of our contributions is presented through an experimental study in simulation, where the 21 DOF manipulator navigates towards regions of inspection within a turbine.

## I. INTRODUCTION

Highly articulated robotic systems have taken several forms over the years - interplanetary and lunar rovers, serpentine robots, and humanoid robots to name a few. Their development has been motivated by the superior mobility they offer when compared to lower dimensional systems. Their capacity for complex and expressive maneuvers have made them attractive choices in several domains including unknown/complex terrain navigation, search and rescue, and inspection [1][2]. While their dimensionality is responsible for their superior mobility, it is the same which makes the tasks of planning for and controlling them difficult.

In this paper, we will focus on developing a path planning algorithm for a 21-DOF snake robot-like manipulator navigating a highly cluttered gas turbine towards regions of inspection. The curse of dimensionality severely cripples the performance of planning algorithms in our problem domain. This is further exacerbated by the extremely constrained environment created by the turbine. Further, even the simple yet essential operations of computing forward kinematics, inverse kinematics, and collision checking for our system are computationally expensive. These reasons call for an in-

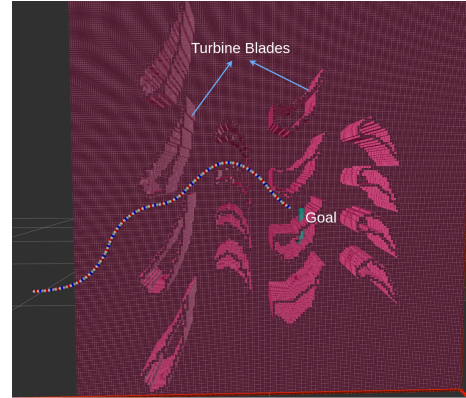


Fig. 1: Snake robot-like manipulator navigating towards an inspection pose within the turbine (indicated by the cyan arrow).

telligent planning algorithm that utilizes domain knowledge to compute feasible paths in a reasonable amount of time.

The overall design of the robot we focus on, as can be seen in Fig. 1. (more details of the design and structure can be found in Section II A) is very similar to a snake robot's design. They share properties like modularity, small cross-section to length ratio, and hyper-redundancy. However, the major distinction between the two stems from the fact that the robot under discussion is not self-propelling. There is an external prismatic actuator that propels the robot. In the past, the term snake robot has been used in the context of self-propelling robots, i.e., robots which locomote purely by changing their shape. This aspect creates significant challenges from the standpoint of controls and there are several works dedicated towards this problem [3] [4]. Since our system is externally propelled while having a design very similar to a snake robot's, we will refer to our system as a snake robot-like manipulator.

The three major classes of planning strategies that are generally adopted for manipulation tasks include - i) Sampling-based strategies [5][6][7] ii) Trajectory Optimization techniques [8][9], and iii) Search-based planning approaches [10]. Although well recognized for their scalability to high-dimensional problems, sampling-based approaches suffer from the narrow passage problem [11] which dramatically inhibits their performance in our domain. The narrow passage problem refers to the poor performance of the sampling algorithms when the free space consists of narrow passages that have to be traversed to reach a goal. From the given model of the turbine we can be confident that there are

<sup>1</sup> M.S. Saleem, R. Sood, and M. Likhachev are with the Robotics Institute, Carnegie Mellon University, Pittsburgh, PA 15213, USA. e-mail: {msaleem2, raghavso, mlikhach}@andrew.cmu.edu.

<sup>2</sup> S. Onodera, R. Arora, and H. Kanazawa are with the Machinery Research Department, Research and Innovation Center, Mitsubishi Heavy Industries, Takasago, Hyogo, Japan.

several narrow passages that need to be navigated to reach regions of inspection. Optimization strategies seem like attractive options as they directly operate in the continuous space. However, using them to plan a long-horizon path for a hyper-redundant system like ours, in an environment riddled with constraints and minimas is extremely time-consuming. The highly cluttered environment in our domain provides excellent reasons for computing an informative heuristic function and using it to guide a search-based planning approach.

The performance of a search algorithm is significantly dependent on the discrete action space chosen and the heuristics used. While the choices for them are straightforward for more traditional problems, a domain such as ours requires careful reasoning. Due to the high clutter in the environment, the high dimensionality, and the joint limit constraints, direct applications of heuristics and action spaces from traditional manipulation domains drive the search into deep minima. Hence, our contributions in this paper are directed towards constructing and utilizing a more suitable action space and heuristics for our problem.

A search-based approach translates planning problems in continuous spaces to search problems in discrete graphs. The graph is constructed by discretizing the continuous action space into a finite set. The effect of this discretization in most manipulation problems is insignificant. However, given the constrained space in our environment there are often situations where a simple predefined action set from a given state is unable to generate valid transitions that can help the search progress.

Our first contribution addresses this issue. We formalize the task of neighbor generation as an optimization problem. This allows us to directly operate in the continuous space of the system overcoming the drawbacks of a discrete action space. Since the problem of generating a neighbor is significantly smaller when compared to solving the planning problem as a whole, the time required for this process is much lesser. At the same time, it is still far too high to be queried for every state encountered within a search (which is typically in the range of hundreds of thousands). To combat this, we introduce optimization-based actions as actions that are invoked *dynamically* on an as-needed basis in addition to the predefined action set (the set of static motion primitives) that is used throughout the search. Due to the computational expense associated with generating the optimization-based actions, they are invoked by the search only when it detects being stuck in a local minima.

The concept of generating motion primitives online for manipulation problems was first introduced in [10]. They refer to such actions as Adaptive Motion Primitives and define them to be actions computed online and always leading to the goal configuration. These were designed to achieve precise positioning at goal configurations which do not necessarily lie on the discretized lattice. However, the goal of optimization-based action is different. It is to overcome the minima created by the discretization. Further, they do not necessarily lead to the goal and are queried at

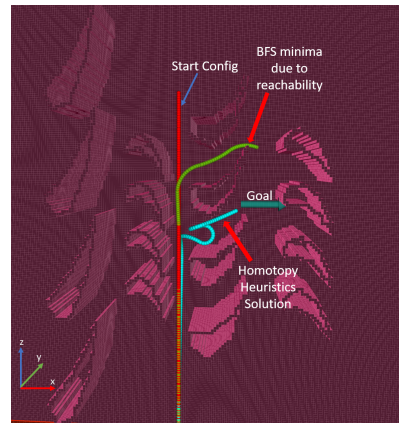


Fig. 2: Minima caused by reachability constraints.

numerous stages within the search.

Our second contribution is the development of a lazy generation strategy which is aimed at further minimizing queries to the optimizer. Inspired from the concept of lazy collision checking [12][13], we have developed a lazy generation strategy which allows us to postpone the actual call to the optimizer for generating an action until absolutely needed. This way the search only queries the optimizer for generating actions that it intends to use (i.e., actions that are potentially part of the solution).

Our final contribution lies in the area of developing an informed heuristic for our problem. Using the solution of a lower-dimensional problem as a heuristic to guide the search in full dimensions is a common approach in the search literature. A good example of this would be to perform a 3D Breadth-First Search (BFS) in the workspace of a manipulator to guide a search in its configuration space [10]. While this is a good heuristic for common manipulation problems it forgoes information about the robot's reachability. A similar approach for our domain would be ineffective due to the extensive reachability constraints present in the system.

Similar problems in other domains like tethered robot planning and humanoid footstep planning have been addressed by the use of topology-based heuristics [14][15]. This class of heuristics reasons about the topological classes induced in the workspace by the obstacles present in the environment. Relevant topological classes for a given planning problem are identified and the search is guided along each of them simultaneously through the use of a Multi-Heuristic framework. We adopt a similar approach for our domain which we outline in the following sections.

## II. PRELIMINARY

### A. Search based Planning

Our search based planning approach is rooted in A\*. A\* finds a path from a start state to a goal state, by repeatedly expanding nodes from a priority list referred to as OPEN. States in the OPEN list are prioritised based on the function  $f(n) = g(n) + h(n)$ . Here,  $g$ -value represents the cost of reaching the state  $n$  from the start state and  $h$ -value otherwise referred to as the heuristic value, is an estimate of

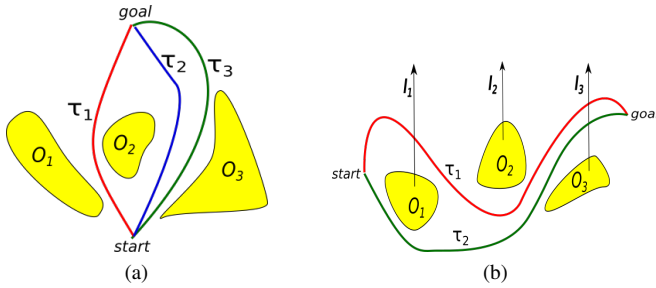


Fig. 3: a) Curves  $\tau_1$  and  $\tau_2$  are in different homotopy classes.  $\tau_2$  and  $\tau_3$  are in the same homotopy class. b) h-signature of  $\tau_1$  is  $l_1 l_3$  and h-signature of  $\tau_2$  is  $l_3$ .

the cost of reaching the goal from  $n$ . The task of expanding a state entails computing the valid successors/neighbors that can be reached from the given state and adding them to the OPEN list based on their priority. Starting with the expansion of the start state, the search terminates when the goal state is expanded. Using the mentioned priority function for the OPEN list guarantees minimal computational effort (as measured by the number of state expansions) to find a provably optimal path to the goal provided the search uses a consistent heuristic.

### B. Homotopy Classes of Curves

Two curves  $\tau_1$  and  $\tau_2$  connecting the same end points are said to be in the same homotopy class if they can be continuously transformed into one another without intersecting any obstacle present in the environment. Continuously deforming curves into one another to determine their respective homotopy classes is a highly non-trivial and expensive operation. This leads us to the functional  $H(\tau)$  a homotopy invariant signature (h-signature) that can uniquely identify the homotopy class of a given curve. There have been different techniques developed over the years to compute this signature [16] [17]. As we reason about homotopy classes in 2-dimensions, we use the reduced word-based method developed in [16], owing to the simplicity of the approach for computing h-signatures of curves defined in 2-dimensional spaces.

To compute the h-signature of a curve, we pick a point on each obstacle  $O_k \in \mathcal{O}$  in the environment and extend a beam  $b_k$  vertically upwards from each of them (until the beam encounters either the boundary of the environment or the boundary of another obstacle  $O_i \in \mathcal{O}$ , whichever comes first). We associate each beam  $b_k$  with a unique letter  $l_k$ . To compute the h-signature of a curve  $\tau$ , we gather the letters of the beams crossed by the path as it progresses from start to goal (in order). If the curve intersects the beam  $b_k$  from one direction (say left-to-right) the letter is recorded as  $l_k$ . And when the curve intersects the beam from the opposite direction (right-to-left) the letter is recorded as  $\bar{l}_k$ . To compute the final h-signature of the curve  $\tau$  we reduce the word by removing continuous occurrences of any letter  $l_k$  and its negation  $\bar{l}_k$ . This reduced word uniquely maps curves to their respective homotopy classes.

## III. PROBLEM FORMULATION

### A. Robot Design

The robot consists of ten flexible units attached to each other through a two-axis revolute joint, allowing the units to yaw and pitch about each other. The first unit is connected to a fixed base through a prismatic actuator which can propel the entire robot ahead. Therefore, the state-space  $\mathcal{S}$  of the ten unit robot is given by  $\{l \times \theta_1 \times \phi_1 \times \theta_2 \times \phi_2 \dots \theta_{10} \times \phi_{10}\}$  where  $l$  is the extension of the base prismatic joint and  $\theta_k$  and  $\phi_k$  are the pitch and yaw angles of  $k^{th}$  unit with respect to the  $k-1^{th}$  unit. Hence, the total degrees of freedom of the system is 21.

Each flexible unit is modeled using 15 rigid cylindrical subunits. The subunits are connected to each other through two axis revolute joints which mimic the joint controlling the unit. Hence, a pitch of  $\theta_1$  in the state-space corresponds to the 15 subunits associated with unit 1 having a pitch of  $\theta_1$  with respect to the previous subunit. Though there are 15 two axis revolute joints associated with each unit, since the joints mimic each other, the degrees of freedom associated with each unit remains 2. The actual hardware design and control of each flexible unit are beyond the scope of this paper.

A camera with a highly constrained field of view is attached to the head of the robot i.e. the tip of the  $10^{th}$  unit and is used for inspecting the turbine.

### B. Problem Statement

The overall goal of the domain is to use the snake robot-like manipulator to inspect regions of interest within a cluttered turbine. Given the environment, let  $\mathcal{S}_{valid}$  represent the space of all valid robot configurations - configurations that are not in collision with the turbine, not self-colliding, and within the joint limits. A transition  $s_i \rightarrow s_{i+1}$  from state  $s_i$  to state  $s_{i+1}$  is said to be valid, if all the intermediate states  $s_{int}$  lie in  $\mathcal{S}_{valid}$ . Since the controller of the system has been designed to linearly interpolate in the joint space, the intermediate states  $s_{int}$  for a transition  $s_i \rightarrow s_{i+1}$  can be obtained by linear interpolation.

If  $\pi$  represents a sequence of states  $\{s_1, s_2 \dots s_t\}$  and  $c(s_i, s_{i+1})$  represents the cost of transition  $s_i \rightarrow s_{i+1}$ ,  $C(\pi)$  represents the sum of the cost of all transitions in the path  $\pi$ . Given a start state  $s_{start} \in \mathcal{S}_{valid}$  and an end-effector goal pose  $q_{goal} \in SE(3)$  within the turbine (from where you can view the regions of interest using the attached camera), the planning problem can be formally stated as to:

$$\begin{aligned} \text{find } \pi^* &= \arg \min_{\pi} C(\pi) \\ \text{s.t. } s_i &\in \mathcal{S}_{valid}, \forall s_i \in \pi && \text{(path of valid states)} \\ s_{int} &\in \mathcal{S}_{valid}, \forall s_i \rightarrow s_{i+1} \in \pi && \text{(valid transitions)} \\ s_1 &= s_{start}, s_t \in \mathcal{S}_G && \text{(start, goal constraints)} \end{aligned}$$

Here  $\mathcal{S}_G$  represents the goal set consisting of robot configurations for which the end-effector pose is at  $q_{goal}$ . For our problem, the cost of a transition  $c(s_i, s_{i+1})$  is defined as the Euclidean distance between the end-effector positions ( $\in \mathbb{R}^3$ ) of the states  $s_i$  and  $s_{i+1}$ .

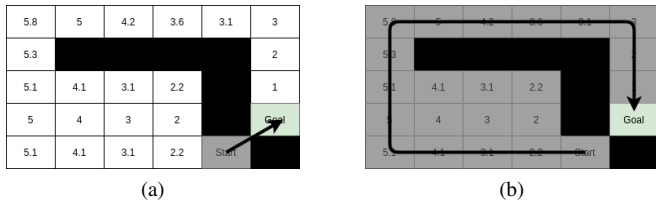


Fig. 4: a) Search terminates in a single expansion with the eight connected action space. b) Search has to expand all the states in the grid with the four connected action space

#### IV. OPTIMIZATION-BASED ACTION

Let us consider the simple example shown in Fig. 4. An agent has to get from the start cell to the goal cell as marked on the grid. Cells completely blacked out are occupied and cannot be transitioned into. The value in every cell represents the heuristic which is the Euclidean distance of the cell from the goal. If we run A\* with an eight connected action set (the agent can transition to any of the immediate neighbor cells including diagonally opposite cells), this problem requires a single expansion. However, when the action set is restricted to four connected and no diagonal moves are permitted, it requires expanding every cell in the grid.

The general discretized action space adopted for the manipulation domain is a set containing small increments and decrements of each joint [10]. For a 21-DOF manipulator, the size of this action set would be 42 ( $2*21$ ). The ideology behind this action set and the action set from the above example is the same. These are barebone primitive actions and combinations of them could result in more complex and useful motions. For example, in the above case the diagonal motion required to reach the goal could be achieved by moving one cell to the right and one cell upwards. However, both the action sets make the assumption that *the barebone primitives result in valid transitions*. And this clearly went awry in the example scenario resulting in significantly more expansions. Since our environment consists of extremely narrow spaces and crevices that need to be navigated, the effect of this assumption is significant in comparison with common manipulation domains.

An example of a minima created by the predefined action set can be seen in Fig. 5. From the given configuration, there exists no action mentioned in the predefined set that helps the robot progress towards the goal. Similar to the state in green, any neighbor that progresses the end-effector towards the goal collides with the environment. Hence, the search spends a large amount of time expanding similar configurations.

A simple solution to this problem would be to add more complex actions to the predefined action set (combinations of the barebone actions). However, for our 21 dimensional system combining pairs of primitive movements alone would result in 420 actions ( $2*21C_2$ ). This is despite disregarding weighting the primitives while combining them (for example an action could involve moving the first joint by 1 unit while moving the second joint by 3 units). Furthermore, given the structure of the robot and the environment, we would require

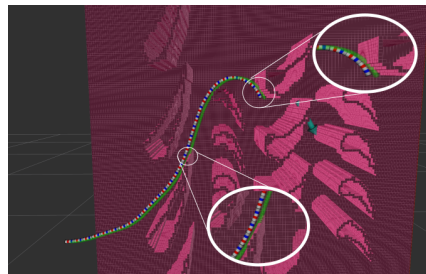


Fig. 5: Example of a minima created by predefined action set. State in green represents a potential neighbor computed using the predefined action set.

combining more than pairs of primitives.

To counter this problem we propose an approach that combines the use of a (sparse) predefined set of actions with the use of optimization-based actions. The latter are constructed dynamically on an as-needed basis, specifically whenever the search encounters local minima, and utilize optimization to compute motions that propel the search out of the minima. Formalizing the generation of a neighbor as an optimization problem allows us to directly operate in the continuous space of all joint angles overcoming the issues encountered by the discrete action space.

Minimas in the search are detected by observing heuristic stagnation [18]. That is, if the heuristic value of the states expanded does not improve over several expansions, it implies that the search is stuck in a local minima. Whenever this occurs, optimization-based actions are generated as additional actions available at the states being expanded.

##### A. Optimization Problem

Let  $s_{min}$  represent the state being expanded while the search is stuck in the local minimum. The goal of the optimization problem is to generate neighbors from  $s_{min}$ . Reasoning about the system in its configuration space is significantly more difficult than reasoning about it in the end-effector space of the robot. There is no direct way to identify configurations in the state space such that moving towards them would help us progress towards the goal. Hence, we choose to define the neighbors to  $s_{min}$  in the end-effector space. This is a natural decision, since the goal of the overall problem is to cause meaningful motions to the end-effector which ultimately results in it reaching the defined goal pose.

Since the end-effector space is  $\mathbb{R}^3$ , like any other 3D domain we can create a simple six connected action set (unit positive and negative motions along each axis). Although a unit motion in the end-effector space seems like a simple task, for the situations encountered in the search, this would require moving potentially all the joints of the robot simultaneously. Hence, for a given  $s_{min}$  we solve six different optimization problems to compute potential neighbors.

To define the optimization problem we need to identify an objective function that will enable reaching a 3D end-effector goal  $g$  from a state  $s$  (which in our case would be  $s_{min}$ ). We formulated an objective that consists of three complementary

components pertinent to our problem - i) Obstacle Cost, ii) Goal Cost, and iii) State Cost.

$$\arg \min_{s' \in \mathcal{S}} \mathcal{F}_{obj}(s, g, s') = \mathcal{F}_{obst}(s) + \lambda \mathcal{F}_{goal}(s, g) + \gamma \mathcal{F}_{state}(s, s') \quad (1)$$

The obstacle cost encourages staying away from the obstacles in the environment by penalizing states that are in collision. This component is very similar to the obstacle cost used previously in [8]. It can be quantified as the inverse of the sum of the distances of every point on the robot from the nearest obstacle. Let  $c_{obst} : \mathbb{R}^3 \rightarrow \mathbb{R}$ , represent the obstacle workspace cost (which is equivalent to a distance field) and  $fk : (s, u) \rightarrow \mathbb{R}^3$ , be the forward kinematics function that returns the workspace position ( $\in \mathbb{R}^3$ ) of a body element  $u \in \mathcal{B}$  for a specific robot configuration  $s \in \mathcal{S}$ . Then the obstacle cost function can be expressed as:

$$\mathcal{F}_{obst}(s) = \frac{1}{\int_{\mathcal{B}} c_{obst}(fk(s, u)) du} \quad (2)$$

The role of the goal cost is to encourage moving towards the goal  $g$ . It is defined as the Euclidean distance in 3D between  $g$  and the end-effector pose of the potential neighbor  $s'$ . If  $u_{ee}$  represents the end-effector

$$\mathcal{F}_{goal}(s', g) = \text{Euclidean}(fk(s', u_{ee}), g) \quad (3)$$

Since the goal for the optimization problem is defined in the end effector space it is important to ensure that the robot does not have to reconfigure itself severely to reach the goal. For this purpose we define the third term of our objective, the state cost. This measures the Euclidean distance between the state in the minima  $s_{min}$  and the potential neighbor  $s'$  in the configuration space. The obstacle cost does not explicitly reason about the validity of the transition itself. Rather, it only tries to ensure that the generated neighbor is collision free. However, this additional term ensures that the reconfiguration is minimal thereby increasing the chances of a valid transition.

$$\mathcal{F}_{state}(s, s') = \text{Euclidean}(s, s') \quad (4)$$

The generated neighbors are checked for collisions and valid transitions from  $s$  before being added as valid successors in the search.

### B. Lazy Generation

Lazy search algorithms are a class of search algorithms developed for domains where the task of edge (transition) evaluation is computationally expensive, thereby acting as the major bottleneck for the planning problem [12][13]. These approaches vie to only evaluate edges that are essential for the search. A good example from this class of algorithms would be Lazy Weighted A\* (LWA\*) [19]. This algorithm postpones evaluating edges until expansion. This way the algorithm only evaluates edges to states that are potentially part of the (bounded sub-)optimal solution.

However, the optimization primitives provide us with the unique opportunity of exploring a different dimension of lazy

---

### Algorithm 1 LAZY GENERATION BASED SEARCH

---

```

1: procedure PLAN( $s_{start}, \mathcal{S}_G$ )
2:    $start.state = s_{start}$ 
3:    $start.g = 0$ ;    $start.h = \text{Heuristic}(start.state)$ 
4:   Insert( $OPEN, start$ )
5:   while  $OPEN$  is not empty do
6:     remove  $s$  with smallest  $f(s)$  from  $OPEN$ 
7:     if pseudostate( $s.state$ ) then
8:        $\hat{s} = \text{queryOptimizer}(s.parent.state, s.state)$ 
9:        $\triangleright$  Generating state corresp. to end effector goal
10:      if validTransition( $s.parent.state, \hat{s}$ ) then
11:         $s.state = \hat{s}$ 
12:         $s.g = s.parent.g + c(s.parent.state, s.state)$ 
13:        Insert( $OPEN, s$ )  $\triangleright$  Reinsert into  $OPEN$ 
14:      continue
15:      if  $s.state$  in  $CLOSED$  then
16:        continue
17:      else if  $s.state \in \mathcal{S}_G$  then
18:        return ExtractPath( $s$ )
19:      else
20:        EXPAND( $s$ )
21: procedure EXPAND( $s$ )
22:   Insert( $CLOSED, s.state$ )
23:    $S' = \text{getSuccessors}(s.state)$   $\triangleright$  Predefined action set
24:   if localMinima then
25:      $S'+ = \text{getOptPseudoSuccessors}(s.state)$ 
26:      $\triangleright$  Returns 3D end effector goals
27:   for  $s' \in S'$  do
28:     if not pseudostate( $s'$ ) then
29:       if validTransition( $s.state, s'$ ) then
30:          $succ.g = s.g + c(s.state, s')$ 
31:       else
32:         continue
33:       else
34:          $succ.g = s.g + \bar{c}(s.state, s')$ 
35:          $\triangleright$  Underestimate of true cost
36:          $succ.state = s'$ ;  $succ.parent = s$ 
37:          $succ.h = \text{Heuristic}(succ.state)$ 
38:         Insert( $OPEN, succ$ )

```

---

algorithms. The bottleneck in this problem is the generation of the optimization primitive rather than collision checking an existing transition (each generation approximately takes 1.5 seconds). Drawing inspiration from LWA\* we choose to delay the generation of the primitive until expansion. Thereby, we query the optimizer only for states essential to the problem.

An outline of the lazy generation based search can be found in Alg. 1. When a local minima in the search is detected, optimization-based actions are queried as additional actions from the state  $s$  being expanded (Line 24). Instead of solving the optimization problems right away and adding the solution states as successors into the OPEN list, we create pseudostates representing the solutions of the optimizer that we add to the OPEN list (Lines 25-38). An optimistic estimate of the cost of transition  $\bar{c}$ , from  $s$  to the potential successor  $s'$  is used to compute the  $g$ -value of the pseudostate (Line 34). Optimistic cost estimate implies that  $\bar{c}(s, s') \leq c(s, s')$ . Only when the pseudostate is selected for expansion, we generate the full configuration of this successor (Line 8). If the transition to this configuration from  $s$  is invalid, we

discard the state and proceed with expanding other states in the OPEN list. If the transition is valid, then we now know the edge’s true cost, so we reinsert it into the OPEN list (Lines 10-14). And when it is popped from the OPEN list the second time, it will actually be expanded and will generate successors of its own. Lazy generation based search similar to LWA\* is both complete and bounded suboptimal.

In our problem domain, both the cost function and the heuristic function are computed in the end-effector space. Hence, both the  $g$ -value and the  $h$ -value of the state can be computed from the end-effector position of the potential neighbor  $s'$  (obtained through the 6 connected grid described in the previous subsection). Hence, there is no requirement for an optimistic estimate of the transition cost.

## V. TOPOLOGY HEURISTICS

The invariance of the turbine environment along the  $y$ -axis (refer Fig. 2 for axes) and the majority of the robot’s transitions lying in the  $x - z$  plane (sideview plane of the turbine) make it sufficient to discuss about topology classes in the 2-D  $x - z$  plane. Choosing a desired homotopy class for a planning problem corresponds to choosing the homotopy class of the 2-D projection of the curve corresponding to the goal configuration. The curves in Fig. 3b in the context of our problem, correspond to the projection of the final configuration of the snake robot-like manipulator.

The obstacles present in the environment and the joint limits present in the system (specifically the prismatic joint) introduce reachability and topological constraints for the robot. Meaning that some goals in the robot workspace can only be reached through specific homotopy classes. Not reasoning about these constraints during the search could lead to scenarios similar to Fig. 2, where the search is directed toward a minima created by the constraint. This calls for a more informed heuristic that reasons about the homotopy classes induced by the blades of the turbine.

The role of the homotopy heuristic is to estimate the cost of reaching the goal pose from any state  $s$  through a specific homotopy class in the projected space. In common manipulation domains when the goal is to compute a heuristic from a state, the distance of the end-effector position of the state  $s$  from the goal pose is estimated. The task here is to estimate the cost of reaching the goal through a specific homotopy class. Hence, the distance of the end-effector of the state to the goal pose through the class of interest is estimated.

Consider the example shown in Fig. 6. Let the curve in red represent the 2-D projection of a state (full robot configuration) for which the heuristic has to be computed. As can be seen in the figure, the curve corresponds to an h-signature of  $l_1$ . Hence, if the desired signature for the final configuration is  $l_1$ , we can estimate the end-effector distance to the goal along the ” ” (empty) signature and use this as the heuristic (which in this case would be  $d_1$ ). If the desired signature for the final configuration is  $l_1l_2$  we can estimate the end-effector distance along the class  $l_2$  (which in this case would be  $d_2$ ).

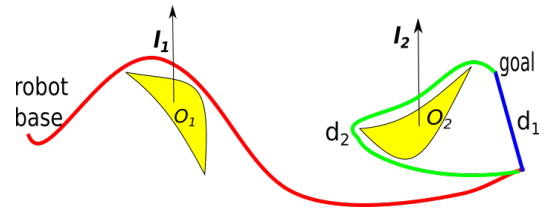


Fig. 6: The curve in red represents the 2D projection of a robot state.  $d_1$  estimates the distance of reaching the goal when the desired class is  $l_1$  and  $d_2$  estimates the distance of reaching the goal when the desired class is  $l_1l_2$ .

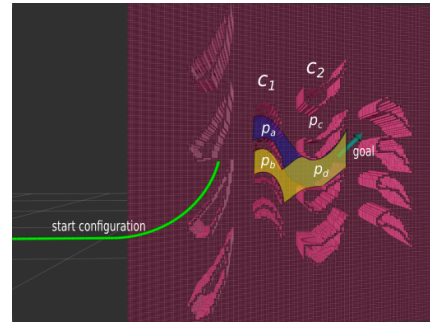


Fig. 7: The goal can be reached from the given start configuration through different passage sequences  $p_a p_d$  and  $p_b p_d$ .

For any state  $s$  encountered in the search, the homotopy heuristic is obtained by computing the distance between the 2D projection of the end effector position of the state  $s_{proj}$  and the projection of the goal pose  $g_{proj}$ , through a homotopy class  $h$ .  $h$  can be obtained by subtracting the signature of the state  $s$  from the desired goal configuration signature. In the example mentioned above, we subtracted  $l_1$  from the desired signature of  $l_1l_2$  and computed the distance along  $l_2$  class. These distances can be obtained by querying the homotopy augmented graph discussed below.

### A. Homotopy Augmented Graph

The goal of this routine is to estimate the distance from points in the 2D projection of the robot workspace to  $g_{proj}$  through specific homotopy classes. For this purpose we do a BFS in a homotopy augmented graph  $G_h$  [16][17] from the node  $(g_{proj}, \text{” ”})$ , where ” ” corresponds to the empty signature. Each vertex in this graph consists of the 2D projection of a point in the workspace and the corresponding h-signature of the path leading up to the point. This additional state variable keeps track of the homotopy of the path from the goal to the current point. Therefore, the distance from any node  $(v, h)$  to the goal node (computed by the BFS), represents the distance from  $v$  to  $g_{proj}$  measured through the homotopy class  $h$ .

### B. Detection of Relevant Homotopy Classes

The obstacles present in the turbine induce multiple topology classes for paths in the robot workspace. We observe that not all of these classes are relevant for a given planning problem. We developed a routine highly specific to the turbine environment that identifies relevant classes. It is also possible to pick these classes through manual inspection.

As can be seen in Fig. 7, the blades of the turbine have been arranged into rows and columns. Consecutive blades in each column define passages through which the robot can traverse. Since it is the obstacles that both induce the homotopy classes and create passages, the problem of identifying a homotopy class of interest can be translated into the problem of identifying a sequence of passages that can be traversed by the robot to reach the goal.

Given a passage  $p$  in a column, it is easy to identify passages in neighboring columns that are closest to  $p$  and can be traversed through, to reach  $p$ . For example, as can be seen in Fig. 7,  $p_d$  in column 2 is reachable through  $p_a$  and  $p_b$  in column 1. Given the start configuration and goal pose, we identify the columns of blades  $\{c_1, c_2..c_n\}$  that need to be traversed by the robot to reach the goal. In the column nearest to the goal pose  $c_n$ , we identify the passage  $p$  closest to the goal that can be used to reach the pose ( $p_d$  in Fig. 7). Once we identify such a passage, we can compute the passage in the previous column  $c_{n-1}$  that can be used to reach  $p$  ( $p_b$  or  $p_a$ ). We repeat this process to identify the passages in all the relevant columns. This sequence of identified passages defines the homotopy class of interest.

Since a passage in any column  $c_n$  can be reached through multiple passages in  $c_{n-1}$  it is possible to identify multiple homotopy classes that could be pursued. It is possible to prioritize sequences based on how close the passages are to each other. For example,  $p_b$  is closer to  $p_d$  in comparison with  $p_a$ . This means that the robot has to travel lesser distance to reach the goal. Thereby, it reduces chances of the search getting stuck in reachability created minimas. Thus, we prefer  $p_b p_d$  over  $p_a p_d$ .

### C. Search

Since there could be multiple promising homotopy classes that the search could be guided along, we use MHA\*, a Multi-Heuristic search framework [20]. This way even if there exists a minima along one of the desired homotopy classes, we could find a solution along the others. MHA\* makes use of multiple OPEN lists, with each list dedicated to a different heuristic function. In our case, this would mean that MHA\* maintains individual OPEN lists for every homotopy class of interest. MHA\* generally employs a round-robin scheduling strategy to choose the OPEN list to expand from, meaning that the search along every homotopy class would be given equal preference. We chose to employ a Dynamic Thompson Sampler (DTS) similar to [21] which would give us the ability to better utilize resources. The DTS approach expands more often from OPEN lists that are more promising and making advances toward the goal. If the search along a specific homotopy class gets stuck in a minima, DTS allocates lesser resources to it and more resources towards a search that is making progress.

## VI. RESULTS

In this section we present the performance of our algorithm through comparisons with sampling based baselines and through ablation studies which help isolate the impact of each

Metric	RRT-Opt	RRT-Search	Ours
Success Rate (%)	20.0	36.6	<b>83.3</b>
Planning Time (s)	277.2	292.3	<b>167.0</b>

TABLE I: Average performance of our approach in comparison with sampling based baselines.

Metric	Predefined + Lazy Opt	Predefined + Opt	Predefined Only
Success Rate (%)	<b>83.3</b>	60.0	20.0
Planning Time (s)	<b>167.0</b>	233.7	300.4

TABLE II: Impact of optimization action.

component of our algorithm. A timeout of 1000 seconds was given for each of the studies, and a failure was recorded if an algorithm was unable to find a solution within the timeout. The results have been averaged over 30 different planning problems. The algorithm used for solving the optimization problem formulated in section IV A as part of our approach, is the stochastic and derivative free black box method of Covariance matrix adaptation evolution strategy (CMA-ES) [22]. Unless explicitly stated, variants of our approach were guided along the top two homotopy classes identified for the problem using techniques described in the previous section.

Table I is a comparative study of our approach against two different versions of RRT [5]. Due to the complexity of the problem, existing baselines like RRT do not work well when directly applied to the problem. Hence, appropriate modifications were made. The sampling for both the RRT baselines in Table I is performed in the 3D workspace of the robot. The difference between the two variants is in the EXTEND routine of RRT which is responsible for extending the nearest neighbor in the tree towards a random sample.

1) **RRT-Opt**: Makes use of the optimizer to implement the EXTEND routine (the same optimizer as used in our own approach). Given a randomly sampled 3D point, it identifies an intermediate point close to the end-effector position of the neighbor and in the direction of the sampled point. It then proceeds to solve the optimization problem we had formulated in section IV A with the intermediate point as the goal and nearest neighbor from the tree as the state from which the neighbor has to be computed ( $s$  in Eqn. 1). If the transition from the neighbor state and the solution of the optimizer has been validated, the process is repeated with a goal closer to the sampled point and the solution of the previous iteration as  $s$ .

2) **RRT-Search**: This variant employs a Weighted A\* search algorithm to extend between the sampled point and

Metric	Two Homotopy with DTS	Two Homotopy w/o DTS	One Homotopy	BFS
Success Rate (%)	<b>83.3</b>	73.3	66.6	23.3
Planning Time (s)	173.9	258.1	197.6	<b>134.7</b>

TABLE III: Impact of homotopy heuristics and DTS.

the neighbor configuration. While utilizing the randomness associated with sampling based approaches, the baseline taps into the effectiveness of search-based techniques as well. We used a simple Euclidean heuristic and an action space similar to the one we had developed for our planner in section IV (including the optimization queries). A timeout of 7 seconds was given for every search query and the state with the minimum heuristic is returned.

Computing inverse kinematic solutions is an expensive process for our 21-DOF system. And the cluttered environment makes it infeasible to sample collision free inverse kinematics solutions from the goal pose. This ruled out the possibility of bidirectional baselines like RRT-Connect [6].

From Table I we see that our approach significantly outperforms the sampling-based baselines. The baselines could solve not more than 36% of the test cases in comparison with the 83% success rate of our approach. The poor performances of the baselines can be primarily attributed to their narrow passage problem discussed in Section I. Outperforming our nearest competitor by solving 50% more problems highlights the significance of our contributions.

Table II and Table III present ablation studies associated with the optimization-based action and topology heuristics respectively. As can be seen in Table II, using just a predefined action set yields a poor success rate. However, the incorporation of the optimization action improves the performance of the planner several fold. It is also visible that the lazy generation technique is a crucial component of our algorithm improving success rate by over 20%.

Table III clearly shows the benefit of using homotopy heuristics over a BFS heuristic. A significant improvement in success rate is observed. It also brings out the trade-off associated with using multiple homotopy heuristics. While having more heuristics slows the search down (as the search has to be guided in multiple directions simultaneously), it increases the overall success rate of the algorithm (as the more relevant directions you guide the search in, the more likely you are to reach the goal without getting stuck in a minima). The table also elicits the impact of using DTS over a round-robin scheduling strategy in the Multi-Heuristic framework.

## VII. CONCLUSION

In this paper the planning problem for a 21 DOF snake-robot like manipulator navigating a cluttered gas turbine was successfully tackled. The minima created by the inadequacy of a discrete action space in the highly constrained turbine environment was tackled through the development of optimization-based actions. Due to the computational expense associated with solving the optimization problem, a lazy generation technique was developed that delays the actual call to the optimizer until absolutely required. The topological constraints created by the blades of the turbine environment and the joint limits, was tackled through the development of homotopy heuristics that reason about the homotopy classes induced in the robot's workspace.

## REFERENCES

- [1] P. Liljeback, O. Stavdahl, and A. Beitnes, "Snakefighter-development of a water hydraulic fire fighting snake robot," in *2006 9th International Conference on Control, Automation, Robotics and Vision*. IEEE, 2006, pp. 1–6.
- [2] A. Selvarajan, A. Kumar, D. Sethu, and M. A. bin Ramlan, "Design and development of a snake-robot for pipeline inspection," in *2019 IEEE Student Conference on Research and Development (SCORED)*, pp. 237–242.
- [3] P. Liljeback, K. Y. Pettersen, Ø. Stavdahl, and J. T. Gravdahl, *Snake robots: modelling, mechatronics, and control*. Springer Science & Business Media, 2012.
- [4] D. S. Rollinson, "Control and design of snake robots," 2014.
- [5] S. M. LaValle *et al.*, "Rapidly-exploring random trees: A new tool for path planning," 1998.
- [6] J. J. Kuffner and S. M. LaValle, "Rrt-connect: An efficient approach to single-query path planning," in *Proceedings 2000 IEEE International Conference on Robotics and Automation. Symposia Proceedings*, vol. 2, pp. 995–1001.
- [7] L. E. Kavraki, P. Svestka, J.-C. Latombe, and M. H. Overmars, "Probabilistic roadmaps for path planning in high-dimensional configuration spaces," *IEEE transactions on Robotics and Automation*, vol. 12, no. 4, pp. 566–580, 1996.
- [8] M. Zucker, N. Ratliff, A. D. Dragan, M. Pivtoraiko, M. Klingensmith, C. M. Dellin, J. A. Bagnell, and S. S. Srinivasa, "Chomp: Covariant hamiltonian optimization for motion planning," *The International Journal of Robotics Research*, vol. 32, no. 9–10, pp. 1164–1193, 2013.
- [9] M. Kalakrishnan, S. Chitta, E. Theodorou, P. Pastor, and S. Schaal, "Stomp: Stochastic trajectory optimization for motion planning," in *2011 IEEE international conference on robotics and automation*, pp. 4569–4574.
- [10] B. Cohen, S. Chitta, and M. Likhachev, "Single-and dual-arm motion planning with heuristic search," *The International Journal of Robotics Research*, vol. 33, no. 2, pp. 305–320, 2014.
- [11] D. Hsu, L. E. Kavraki, J.-C. Latombe, R. Motwani, S. Sorkin *et al.*, "On finding narrow passages with probabilistic roadmap planners," in *Robotics: the algorithmic perspective: 1998 workshop on the algorithmic foundations of robotics*, 1998, pp. 141–154.
- [12] A. Mandalika, S. Choudhury, O. Salzman, and S. Srinivasa, "Generalized lazy search for robot motion planning: Interleaving search and edge evaluation via event-based toggles," in *Proceedings of the International Conference on Automated Planning and Scheduling*, vol. 29, 2019, pp. 745–753.
- [13] C. Dellin and S. Srinivasa, "A unifying formalism for shortest path problems with expensive edge evaluations via lazy best-first search over paths with edge selectors," in *Proceedings of the International Conference on Automated Planning and Scheduling*, vol. 26, 2016.
- [14] S. Kim, S. Bhattacharya, and V. Kumar, "Path planning for a tethered mobile robot," in *2014 IEEE International Conference on Robotics and Automation (ICRA)*, pp. 1132–1139.
- [15] V. Ranganeni, O. Salzman, and M. Likhachev, "Effective footstep planning for humanoids using homotopy-class guidance," in *Proceedings of the International Conference on Automated Planning and Scheduling*, vol. 28, no. 1, 2018.
- [16] V. Narayanan, P. Vernaza, M. Likhachev, and S. M. LaValle, "Planning under topological constraints using beam-graphs," in *2013 IEEE International Conference on Robotics and Automation*, pp. 431–437.
- [17] S. Bhattacharya, M. Likhachev, and V. Kumar, "Topological constraints in search-based robot path planning," *Autonomous Robots*, vol. 33, no. 3, pp. 273–290, 2012.
- [18] F. Islam, O. Salzman, and M. Likhachev, "Online, interactive user guidance for high-dimensional, constrained motion planning," *arXiv preprint arXiv:1710.03873*, 2017.
- [19] B. J. Cohen, M. Phillips, and M. Likhachev, "Planning single-arm manipulations with n-arm robots," in *Robotics: Science and Systems*, 2014.
- [20] S. Aine, S. Swaminathan, V. Narayanan, V. Hwang, and M. Likhachev, "Multi-heuristic a," *The International Journal of Robotics Research*, vol. 35, no. 1–3, pp. 224–243, 2016.
- [21] M. Phillips, V. Narayanan, S. Aine, and M. Likhachev, "Efficient search with an ensemble of heuristics," in *Twenty-Fourth International Joint Conference on Artificial Intelligence*, 2015.
- [22] N. Hansen, "The cma evolution strategy: A tutorial," *arXiv preprint arXiv:1604.00772*, 2016.